Organic & Biomolecular Chemistry

PAPER

View Article Online
View Journal | View Issue

Cite this: *Org. Biomol. Chem.*, 2014, **12**, 4479

Proline *N*-oxides: modulators of the 3D conformation of linear peptides through "NO-turns"†‡

Majid D. Farahani,[a] Bahareh Honarparvar,[a] Fernando Albericio,[a,b,c] Glenn E. M. Maguire,[a,b] Thavendran Govender,[a] Per I. Arvidsson*[a,d] and Hendrik G. Kruger*[a]

Received 25th February 2014,
Accepted 9th April 2014

DOI: 10.1039/c4ob00433g

www.rsc.org/obc

Small peptides are essential mediators of numerous physiological processes. Consequently, there is huge interest in the *de novo* design of peptides with a predictable folding and related biological activity. In this study, we investigate the possibility of modulating the secondary structure of tetrapeptides through proline *N*-oxide moieties and N-methylation of the peptide backbone. A series of tetrapeptides were synthesised to investigate the combined effect of Pro *N*-oxide and N-methylation of the amide bond on the (n + 1) residue in terms of *cis*- and *trans*-isomerization, as well as how these modifications direct potential intramolecular hydrogen bonding interactions. The right combination of both these parameters led to a *trans* to *cis*-conformational interconversion and a change in the nature of the hydrogen bonding interactions, as demonstrated by NMR spectroscopic, molecular modeling analysis and thermal coefficient studies. Proline *N*-oxide residues were proposed to induce turns we named as NO-γ-turns and NO-β-turns based on their similarity to traditional γ- and β-turns.

Introduction

During the last few years, the number of peptide-based pharmaceutical drugs reaching the market has notably increased.[1] Peptide-based drugs have many advantages, such as high potency, and they often display a more limited off-target side-effect profile than traditional small molecule drugs.[2] However, the oral bioavailability of peptides is a major obstacle that hinders the development of more therapeutic formulations.[3–5] Pharmacokinetic properties such as short plasma half-life and sensitivity to enzyme degradation, as well as the tendency to undergo aggregation are some of the main reasons for their low bioavailability.[3,6,7]

Selective N-methylation of amide nitrogen atoms[8–10] increases the proteolytic stability/bioavailability.[11] It also dramatically increases the aqueous solubility of the peptide,[11] whilst simultaneously increasing the lipophilicity[10] and the conformational rigidity of such peptides.[8–10]

Proline residues are important inducers of peptide folding, yielding secondary structures with β-turn or alpha helix character.[12–18] The proline amide bond displays a relatively high *cis–trans* isomerization ratio (3–5% *cis*-isomers).[19–25] The rotational energy barrier for proline *cis*/*trans*-amide isomerization is normally in the range of 16–20 kcal mol^{-1} (ref. 26) which is on the border of being achievable at room temperature; however, values as low as 8 kcal mol^{-1} have been recorded.[27,28] A change in *cis*/*trans*-isomerization ratio can be of fundamental importance for controlling peptide folding.[29,30]

The synthesis of structurally constrained peptides can be achieved with several strategies, the most popular being cyclisation of the peptide.[31,32] Synthesis of self-assembled peptides utilizing van der Waals forces, hydrogen bonds, hydrophobic and aromatic π–π stacking is another way to form secondary structures, such as turns, helices, and sheets.[33–40] A γ-turn[41] and a β-turn[41–50] are presented in Fig. 1.

Proline is known to be an active β-turn inducer when placed in the (i + 1) position in peptide backbones. In an effort to find alternative sources of β-turn inducers, our group has previously reported various cage peptides.[50–52] Herein, we present

[a]*Catalysis and Peptide Research Unit, School of Health Sciences, University of Kwazulu-Natal, Durban 4001, South Africa*
[b]*School of Chemistry and Physics, University of Kwazulu-Natal, Durban 4001, South Africa*
[c]*Department of Organic Chemistry, University of Barcelona, 08028 Barcelona, Spain*
[d]*Science for Life Laboratory, Drug Discovery & Development Platform & Division of Translational Medicine and Chemical Biology, Department of Medical Biochemistry and Biophysics, Karolinska Institutet, Stockholm, Sweden.*
E-mail: kruger@ukzn.ac.za, per.arvidsson@scilifelab.se

†In memory of Professor Per Ahlberg, leading physical organic chemist and mentor.

‡Electronic supplementary information (ESI) available: NMR assignments for each compound, NMR-based thermal coefficient graphs, and NMR and HRMS spectra. See DOI: 10.1039/c4ob00433g

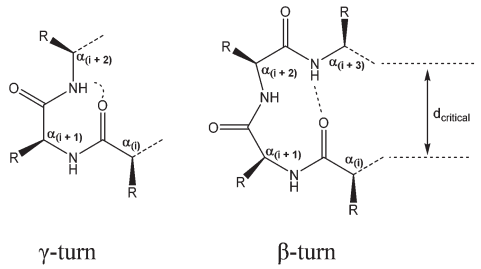

Fig. 1 Criteria used in the identification of γ- and β-turn characteristics.[41,46,50]

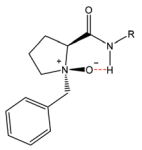

Fig. 2 Proposed *N*-oxide hydrogen bonding arrangement by O'Neil and co-workers.[54]

a new tool to form β-turns by taking advantage of the capability of the *N*-oxide moiety to form strong hydrogen bonds when introduced into proline.

O'Neil and co-workers studied the conformational effect of proline *N*-oxides [P(NO)] using either *N*-alkyl-P(NO)-amide or *N*-alkyl-P(NO) containing dipeptides and showed that hydrogen bonding takes place mainly through a six-membered ring (Fig. 2). In addition it was reported that the formation of hydrogen bonds between amide protons further away from (*i* + 2) and the *N*-oxide is unlikely and, if formed, bonds would be quite weak.[53,54] The stereochemistry of the oxygen atom is well established.[53,54] Attack of the oxygen on this system occurs exclusively from the same side as the amide group due to the hydrogen bonding interaction between the amide and the chloroperbenzoic acid (*m*-CPBA).

The observed "NO-γ-turn" consists of 6 atoms and cannot be classified as a classic γ-turn with 7 atoms (see Fig. 1).

We therefore decided to develop a new concept of peptide "NO-turns" based on the presence of tertiary *N*-oxide moieties, with or without selective N-methylation. The scope and limitations of this concept as modulators of tetrapeptide conformations are reported.

Results and discussion

Two different families of peptides were earmarked. The sequence of the first was chosen based on a high probability for β-turn formation and the second with amino acids known *not* to induce turns. Several tetrapeptides, containing *N*-oxide-*N*-benzylproline as the N-terminal residue (Fig. 3), were prepared. For the first peptide family we chose [Bz(NO)PGNF]. Asparagine (N) and phenylalanine (F) are also known to assist with turn formation.[55,56] For the second peptide family we

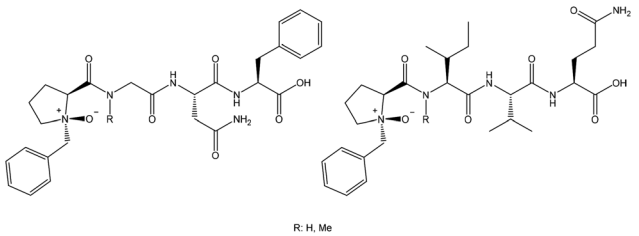

Fig. 3 *N*-Oxide-proline tetrapeptides. [Bz(NO)PGNF], [Bz(NO)PMeGNF], [Bz(NO)PIVQ] and [Bz(NO)PMeIVQ].

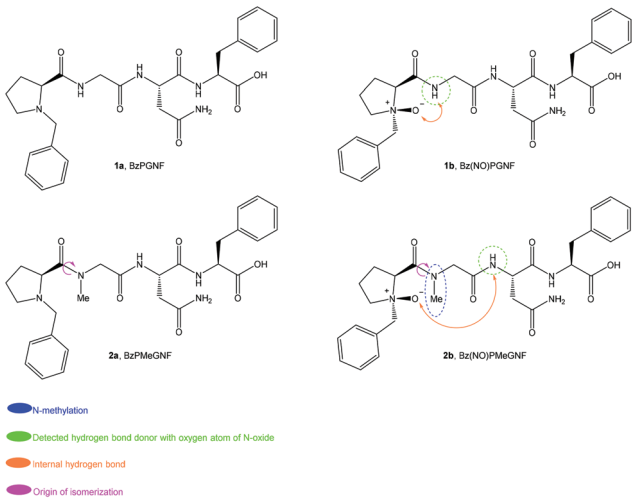

Fig. 4 Peptides theoretically designed for optimal β-turn characteristics.

selected [Bz(NO)PIVQ]. Both isoleucine (I) and valine (V) are known to prevent β-turn formation of short peptides.[55–58] Glutamine was chosen as the final residue since it is bulkier than asparagine. Control peptides without the *N*-oxide were also synthesised. In the next level of this study, the first residues were replaced with N-methylated amino acids to investigate the possibility of obtaining a wider turn. The conformational preferences of the designed *N*-oxide peptides were studied by NMR spectroscopy, including NOE experiments[59,60] as well as molecular modeling.

In the case of the *N*-oxide and N-methylated peptides, potential hydrogen bonding interactions between the (*i* + 2) amide proton and the *N*-oxide group is a possibility. Such a "NO-β-turn" has 9 atoms (Fig. 4) and cannot be classified as a classic β-turn with 10 atoms (Fig. 1).

Peptides were synthesized *via* a solid-phase approach on 2-chlorotrityl-chloride (CTC)-resin with HBTU/DIEA as a coupling cocktail using Fmoc protection of the amino groups. For better control of the synthetic process, previously prepared *N*-benzylproline was incorporated as the last building block.[61] At the end of the synthesis the peptides were cleaved from the resin with 40% TFA in DCM and the tertiary amine of the proline was stereoselectively oxidized[62,63] using *m*-CPBA and K_2CO_3 in DCM at −72 °C (Scheme 1). Peptides were purified *via* semi-preparative HPLC with a C_8 column and the struc-

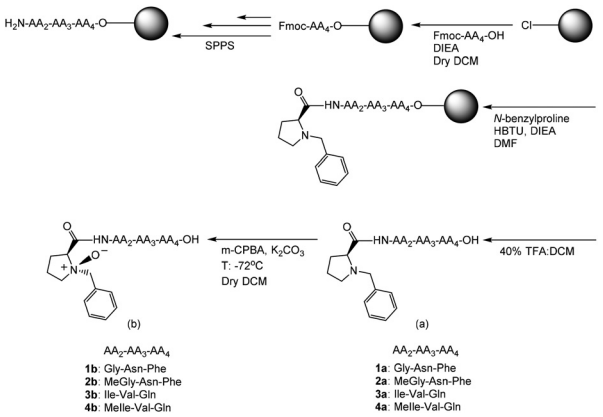

Scheme 1 Synthetic strategy used to prepare the proposed peptides.

tures were characterized by NMR and HRMS. The HPLC chromatogram presents a single peak for each compound, despite the different conformations observed by NMR. No sign of epimerization of the peptides was observed.

Comparative structural study on the peptides designed for optimal β-turn characteristics

The four structures in the first family of peptides are presented in Fig. 4. NMR techniques were employed to identify the proline *N*-oxide peptides and to determine the conformational preferences and stabilities of these series of molecules. Complete NMR assignments of all peptides were performed through 2D NMR techniques. These assignments are presented in the ESI.‡ Three aspects were monitored: (a) the ratio of *cis*/*trans* isomerization, (b) deshielding of the amide protons (NH) due to through space deshielding by the NO oxygen and (c) potential NOE interactions characteristic of β-turns.

The *cis*/*trans* ratio was calculated from the integration of unique proton signals (such as the N-methyl protons). A summary of these results is presented in Table 1.

From the NMR data, no *cis* conformation was observed for peptides **1a** or **1b**, while it was clear that at least two dominant conformations were present for peptides **2a** (47 : 53) and **2b** (29 : 71). Introduction of the *N*-oxide does not lead to epimerization as is demonstrated from the NMR spectra for compounds **1b** and **3b**. Also, if epimerization of the same proton had occurred, then the ratio should have moved closer to 50 : 50 and not further away as is the case for **2b** (29 : 71). If epimerization of other α-protons had taken place, then more complex peak splitting should have been observed for **2b**. Therefore, these conformations are ascribed to *cis*/*trans* isomers of the N-methylated peptide bonds, as shown in Fig. 4. Interestingly, individual cases have been reported where certain proline containing peptides gave up to 50% and also complete *cis*-conformations.[60,64–78] However, there is no definite rule with respect to the equilibrium of *cis*- and *trans*-isomers of peptides, but solvent polarity plays a prominent role. A polar solvent, such as DMSO with a large dipolar moment (3.96 D), favours *cis*-isomers, while less polar solvents, such as water (1.85 D), induce more *trans*-character.[79,80]

The *cis*/*trans* ratio around the amide bond increases through N-methylation.[81–84] There appears to be no particular rule that governs the ratio of *cis*- and *trans*-conformations of N-methylated peptides. The population of *cis*-isomers is generally higher at lower temperatures, but decreases at room temperature,[85,86] this equilibrium being highly dependent on the local environment, such as peptide backbone and solvent.[80,85,87] Energy barriers between 15 and 20 kcal mol^{-1} can be overcome at room temperature[88,89] and the energy barrier of amide rotation for N-methylated peptides is slightly lower than that,[28,90] confirming our conclusion about *cis*–*trans* conformations of the N-methylated peptides.

Comparison between compounds 1a and 1b. Peptide **1a** displayed only the *trans*-isomer. After assigning each peak in ^{1}H NMR and 2D NMR, it seemed that this peptide assumed an extended or linear conformation; none of the NMR data supported a turn structure.

The *N*-oxide peptide **1b** appeared as two conformers (major and minor). Since introduction of the *N*-oxide was proven to be stereo-selective,[53,54] we ruled out the possibility of diastereomers. ROESY NMR data indicated that both conformers are *trans* with respect to the amide bonds (available in the ESI‡).

It should be noted that the percentage of minor conformations in **1b** was quite small (15%), hence only a weak NOE interaction was observed for this conformer. An analysis of these two conformations was performed from the NMR data and is presented in Fig. 5.

The ^{1}H NMR data suggest that the first amide proton (i + 1) of the major isomer of **1b** prefers to engage with the *N*-oxide moiety, thus forming the NO-γ-turn. This is evident from the downfield shift of the (i + 1) amide proton with respect to **1a** in the proton NMR spectra. This shift is most likely the result of an intramolecular hydrogen bonding interaction between the amide proton and the *N*-oxide oxygen atom, causing through space deshielding and suggests the presence of the projected NO-γ-turn. The minor conformation exhibited a more extended structure. The variable temperature NMR data indicated that the major isomer (NO-γ-turn) converts to a more extended conformation at higher temperatures (Fig. 6).

The fact that the major product of **1b** converts to the minor product upon heating from 293 K to 303 K confirms our conclusion that the splitting of these proton signals is due to a conformational issue (*cis*–*trans*-conformation of N-methylated peptides) and as a result of epimerization or diastereomeric effects from non-stereospecific N-oxygen addition.

Table 1 *cis*–*trans* Isomerizations of proline amide bonds at the C-termini of peptides **1** and **2** at room temperature. Data obtained from proton NMR integrations in DMSO-d_6

Peptide	Sequence	*cis* %	*trans* %
1a	BzPGNF	0	100
1b	Bz(NO)PGNF	0	100[a]
2a	BzPMeGNF	47	53
2b	Bz(NO)PMeGNF	29	71

[a] This sequence shows two conformations (see Fig. 5).

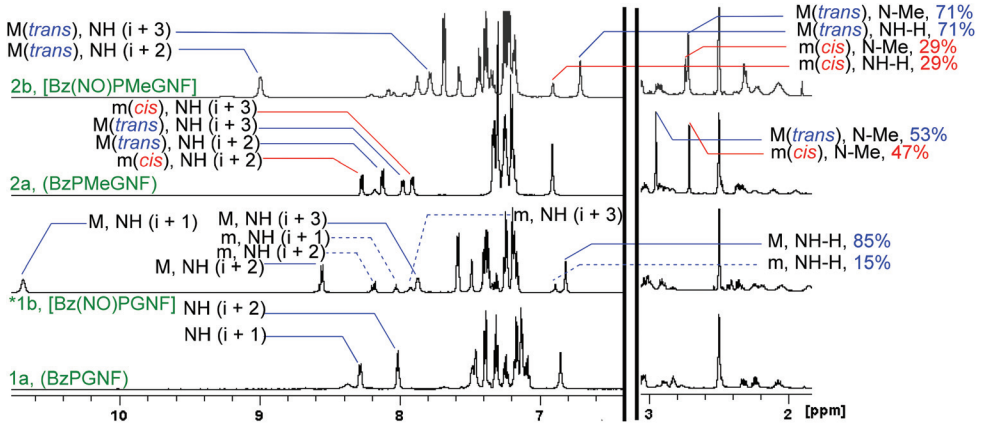

Fig. 5 Downfield region of ^{1}H NMR of designed peptides for optimal β-turn characteristics. The spectra were obtained at room temperature and DMSO-d_6 was used as the solvent. (Blue = *trans*-isomer, red = *cis*-isomer, M = major and m = minor). *Two conformations were observed. The major conformation appeared to exhibit NO-γ-turn character (prominent (i + 1) NH and NO interaction). The minor conformation is possibly a more extended peptide conformation (lack of NH and NO (i + 1) interaction).

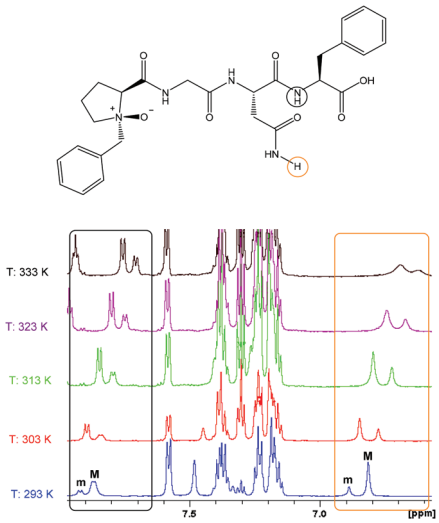

Fig. 6 Thermodynamic study of peptide **1b**, [Bz(NO)PGNF]. Chemical shifts are reported in ppm. The major (M) product converts to the minor (m) product with increasing temperature (solvent: DMSO-d_6).

Table 2 NOE correlations for *trans*-**2b** at room temperature in DMSO-d_6, [Bz(NO)PMeGNF]

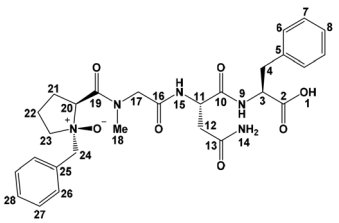

Atom number	Correlated hydrogen atoms
18	15
21	11, 14, 15, 26
22	17
26	17,20

Comparison between compounds 2a and 2b. Peptide **2a** includes N-methylated glycine as the first amino acid following *N*-benzylproline. As expected, both *cis*- and *trans*-isomers exist and the isomerization ratio is 47 : 53 at room temperature (Fig. 5).

The isomers were verified from the ROESY data (available in the ESI‡). It is clear that the *trans*-conformation should experience a through space NOE interaction between the proline Hα and the methyl protons (*N*-Me). This was absent for the *cis*-isomer due to the methyl protons (*N*-Me) pointing in the opposite direction.

The complete NMR elucidation of the *cis*-isomer could not be achieved due to a low signal to noise ratio and overlapping of signals with the *trans*-isomer. Still, it is clear that the *cis*-isomer (29%) was not involved in any hydrogen bonding interaction (Fig. 5).

Peptide **2b** is mainly present as a *trans*-isomer (71% population); the backbone amide proton of asparagine (i + 2) was de-shielded (about 9 ppm) due to the proposed interaction with the *N*-oxide oxygen (Fig. 5) which causes a moderate hydrogen bonding interaction. This result suggests that the *N*-oxide moiety can be used as a kind of β-turn inducer leading to formation of the new NO-β-turn, as confirmed by correlations in the ROESY NMR spectra (Table 2).

ROESY data for *trans*-**2b** are presented in Table 2. The correlations of H-21 with H-11, H-14 and H-15 as well as the correlations of H-26 with H-20 and H-17 provide convincing proof of the presence of a NO-β-turn in **2b**. These correlations suggest that the intramolecular hydrogen bonding interaction between NO and the backbone asparagine NH is able to induce folding of the peptide (Table 2).

Comparison between compounds 1b and 2b. When the first hydrogen bond donor in the position (i + 1) is blocked with a methyl group as in the case of **2b**, the possibility of hydrogen bonding between the amide group (i + 1) and the *N*-oxide moiety is eliminated. Thus, the inherently strong NO-γ-turn preference can be overcome through the introduction of an *N*-Me amino acid that forces the peptide to adopt the novel

NO-β-turn "by design". The shielding effect of the NO on the corresponding amide NH protons (i + 2) can be seen in Fig. 5. For **1b**, the hydrogen bonding interaction between the amide proton of glycine (i + 1) and the negative NO oxygen at the N-terminal of proline provides a stronger deshielding interaction, compared to the amide proton (i + 2) of the more distant asparagine and NO.

Comparative structural study on peptides designed for minimal β-turn characteristics

The four structures in the second family of peptides are presented in Fig. 7. Complete NMR assignments for all peptides were performed utilising 2D NMR techniques. These assignments are presented in the ESI.‡ As expected, only *trans*-amide conformations were observed for the non-methylated peptides **3a** and **3b**. The NMR spectra of **3b** clearly demonstrate that epimerization does not occur upon introduction of the *N*-oxide.

At least two conformations were presented for peptides **4a** and **4b**. As argued for **2a** and **2b**, these split NMR signals are being ascribed to *cis*–*trans*-isomers of the N-methylated peptide bonds, as illustrated in Fig. 7. A summary of these results is presented in Table 3.

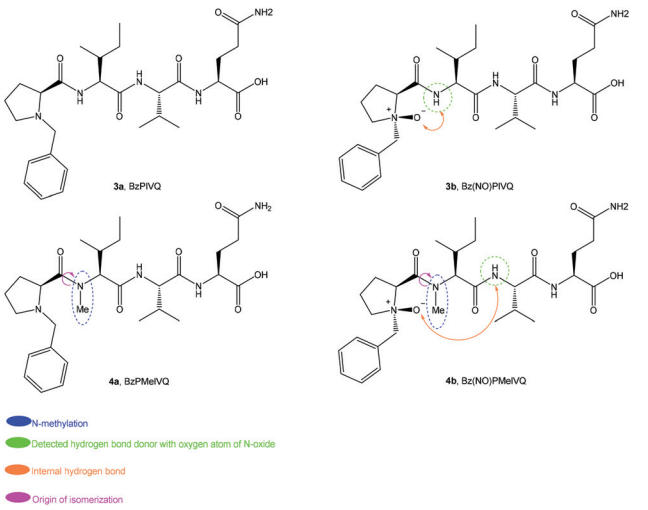

Fig. 7 Peptides designed for minimal formation of β-turn characteristics.

Table 3 *cis*/*trans* Isomers of the proline amide bonds at the C-termini at room temperature. Data obtained from proton NMR integrations are in DMSO-d_6

Peptide	Sequence	*cis* %	*trans* %
3a	BzPIVQ	0	100
3b	Bz(NO)PIVQ	0	100
4a	BzPMeIVQ	40	60
4b	Bz(NO)PMeIVQ	77	23

Comparison between 3a and 3b. Comparisons of the NMR chemical shifts for NH in the (i + 1) positions were made. A 4 ppm difference is found between the isoleucine amide proton signals (Fig. 8; in peptide **3a** this NH appears at 7.85 ppm and in **3b** at 12.05 ppm). This strong through-space deshielding effect was a clear indication of a strong hydrogen bonding interaction between the NH (i + 1) proton and the negatively charged NO oxygen atom. These results are in agreement with the report by O'Neil *et al.*,[53,54] and mark the presence of a NO-γ-turn.

In order to analyse the versatile nature of this NH to NO hydrogen bonding interaction, N-methylation of the isoleucine amide nitrogen (i + 1) was carried out. When peptide **1b** is compared with peptides **3a** and **3b**, it appears that the flexible nature of glycine in the peptide backbone and the absence of a chiral centre cause the hydrogen bonding interaction between the *N*-oxide oxygen and the amide proton to be less prominent in **1b** despite the known turn-inducing element Pro-Gly.

Comparison between 4a and 4b. From Table 4, it is proposed that N-methylation induces *cis*-isomers for both peptides. The presence of the *cis*-isomer for **4a** in a 40% ratio is favoured by the polar NMR solvent (DMSO-d_6). The *trans*-isomer was recognized as the major conformer in the proton spectrum (60%) at ambient temperature (Fig. 8). Both isomers were observed in a ROESY NMR experiment (available in the ESI‡).

Further investigations were conducted to observe if any folding occurred in peptide **4a**. No extraordinary ROESY

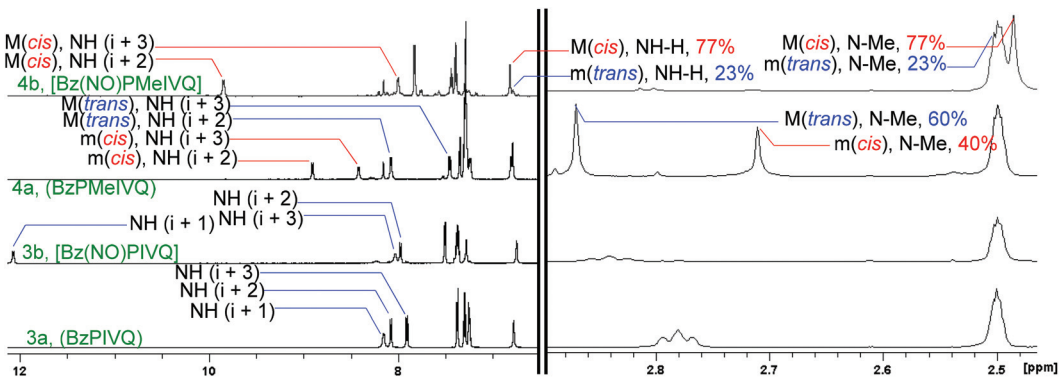

Fig. 8 Downfield region of ^{1}H NMR of designed peptides for minimal β-turn characteristics. The spectra were obtained at room temperature and DMSO-d_6 was used as the solvent.

Table 4 NOE correlations of *cis*-**4b**, [Bz(NO)PMeIVQ], at room temperature in DMSO-d_6

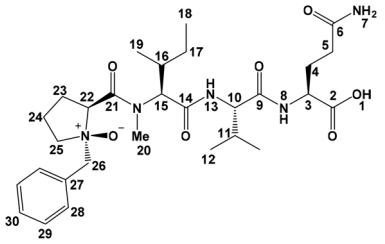

Atom number	Correlated hydrogen atoms
20	12, 16, 17, 18
24	12
26	15
28	13

correlations were observed; it was therefore concluded that neither of the backbones are involved in any stable turn or fold. The NMR spectra of **4b** also presented multiple isomers. The ratio could not be accurately established from protons of the methyl group of the *N*-Me group due to overlap; however, the glutamic acid side chain amide protons revealed an unexpected 77 : 23 *cis*/*trans*-ratio in favour of the *cis*-isomer (Fig. 8). The isomer assignments were confirmed when it was established that the NH proton of valine (i + 2) at about 9.9 ppm experienced through space deshielding due to the proposed intramolecular hydrogen bonding with the *N*-oxide moiety (Fig. 8). Further evidence for this elucidation was obtained from the ROESY spectra of **4b** (available in the ESI‡).

We initially chose isoleucine and valine residues because they have been reported to prevent β-turns.[55–58] The turn observed in the peptide *cis*-**4b** appears to be a new NO-β-turn, created by the *N*-oxide moiety in the presence of these residues. To the best of our knowledge this is the first example of such a secondary structure involving this sequence. Development of a NO-β-turn secondary structure in the presence of bulky amino acids, such as isoleucine and valine, is therefore a novel and unique achievement, and appears to only occur as a result of the (NO)P in the peptide backbone.

The NO-β-turn character of *cis*-**4b** was confirmed with several long-range correlations from ROESY NMR spectra, as demonstrated in Table 4. Convincing evidence for the presence of a NO-β-turn in **4b** is: (a) correlations of H-20 with H-12, H-17 and H-18, (b) a correlation between H-23 and H-12 and (c) a relation between H-24 and H-12, (d) the existence of NOE correlations between H-26 and H-15, H-17 and H-18, and (e) a correlation between H-28 and H-12. These correlations support the presence of intramolecular hydrogen bonding interactions between the backbone asparagine NH and NO, which induced folding of the peptide though the NO-β-turn.

Comparison between 3b and 4b. The potential of the *N*-oxide group to induce hydrogen bonding can be clearly seen in **3b** and **4b** (Fig. 7). The amide proton of isoleucine (i + 1) in **3b** appeared at about 12 ppm, whereas the amide of valine (i + 2) in **4b** appeared at approximately 10 ppm (Fig. 8). This result indicates a relatively close distance between the hydrogen bond donor (i + 2) and the acceptor (*N*-oxide) in the case of **4b**. An even stronger hydrogen bond between the closest amide and NO in peptide **3b** was evident from the large deshielding effect on the (i + 1) amide proton (Fig. 8). The *trans*-conformation of **3b** and the steric hindrance imposed by isoleucine and valine appeared to prevent any interaction between the other amide protons and the NO. In contrast, the *N*-oxide moiety in **4b** revealed a 77% *cis*-conformation which was able to overcome this difficulty of inducing hydrogen bonding between NH (i + 2) and NO.

Thermal shift coefficient NMR investigation: the nature of the hydrogen bonding interaction between the proline *N*-oxide and the backbone NH protons

As discussed before, the presence of this hydrogen bond can be detected by observing the chemical shifts of backbone amide protons in the ^{1}H NMR spectra. Furthermore, an analysis of the thermal behaviour of hydrogen bonds in the peptides by NMR is an elegant technique to study the exact nature of this interaction.[91–96] Normally the intramolecular hydrogen bonding interaction between a hydrogen bond donor (amide proton) and an acceptor (carbonyl oxygen) in a peptide is disturbed at higher temperatures; the amide proton signals also experience a downfield shift (less through space deshielding) in the ^{1}H NMR spectra in aprotic solvent systems.[91–96] In aprotic solvents such as DMSO-d_6, when $-\Delta\delta/\Delta T > 5^1$ ppb K^{-1}, the typical intramolecular peptide hydrogen bonding is absent if the amide protons are solvent-exposed. When $-\Delta\delta/\Delta T < 3$ ppb K^{-1} the amide proton is shielded from the solvent, due to hydrogen bonding with any carbonyl oxygen atom.[91–96]

The plotted $-\Delta\delta/\Delta T$ graphs (available in the ESI‡) for peptides and N-methylated peptides in DMSO-d_6 confirmed that no intramolecular hydrogen bonds exist for peptides **1a–4a**. The presence of hydrogen bonds between the NO moiety and hydrogen-bonded NH in different *N*-oxide peptides **1b–4b** was also investigated with this method. These molecules present a low $-\Delta\delta/\Delta T$ value (−2.64 to 0 ppb K^{-1}) for amide protons involving hydrogen bonding with the *N*-oxide moiety. When these amide protons are not involved in hydrogen bonding interactions, the values are >4 (ppb K^{-1}). The results for peptides **1b–4b** are presented in Fig. 9–12. The negative value for $-\Delta\delta/\Delta T$ (which renders positive slopes) called for a more in depth analysis.

Langner and Zundel[97] reported that in acid–base equilibria (AH···B$^-$ ⇔ A$^-$···HB), where ΔpK_a is defined as [pK_a B − pK_a AH],[98,99] in systems with an increasing ΔpK_a, the proton from the hydrogen bond donor moves closer to the acceptor, which causes deshielding of the mentioned proton. These results are also consistent with an entropy (S) argument and shifting of the proton in this system is due to increase in the amount of the negative entropy.[97]

The hydrogen bond donor (AH) in this study was hydrogen-bonded amides and the acceptor's (B) role was played by the *N*-oxide moiety. The proton chemical shift for several of these

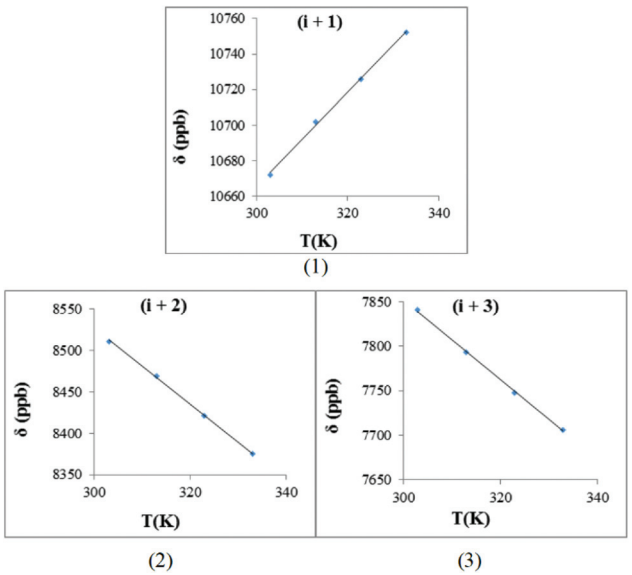

Fig. 9 The hydrogen bond investigation with thermal coefficient plots for each amide protons of *trans*-**1b**, [BzP(NO)GNF]. (Solvent: DMSO-d_6), (temperature: 293–333 K): (1) HN-Gly ($-\Delta\delta/\Delta T$ = −2.64 ppb K^{-1}), (2) HN-Asn ($-\Delta\delta/\Delta T$ = 4.56 ppb K^{-1}), (3) HN-Phe ($-\Delta\delta/\Delta T$ = 4.50 3 ppb K^{-1}) (R^2 > 0.997 for all graphs).

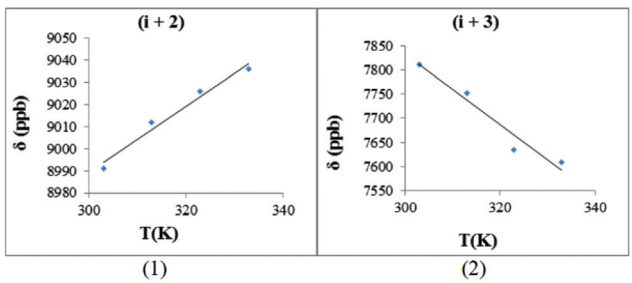

Fig. 10 The hydrogen bond investigation with thermal coefficient plots for each amide protons of *trans*-**2b**, [Bz(NO)PMeGNF]. (Solvent: DMSO-d_6), (temperature: 293–333 K): (1) HN-Asn ($-\Delta\delta/\Delta T$ = −1.49 ppb K^{-1}), (2) HN-Phe ($-\Delta\delta/\Delta T$ = 7.29 ppb K^{-1}) (R^2 > 0.951 for all graphs) (graphs for *cis*-**2b** are available with the ESI‡).

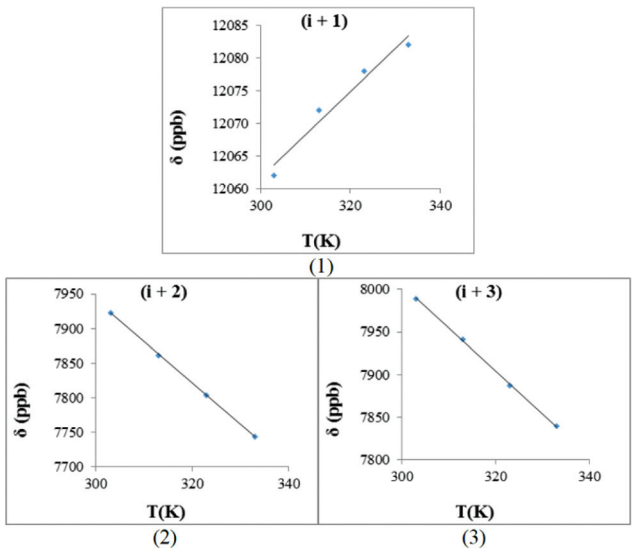

Fig. 11 The hydrogen bond investigation with thermal coefficient plots for each amide of *trans*-**3b**, [Bz(NO)PIVQ]. (Solvent: DMSO-d_6), (temperature: 293–333 K): (1) HN-Ile ($-\Delta\delta/\Delta T$ = −0.66 ppb K^{-1})^4, (2) HN-Val ($-\Delta\delta/\Delta T$ = 5.98 ppb K^{-1}), (3) HN-Gln ($-\Delta\delta/\Delta T$ = 5.04 ppb K^{-1}) (R^2 > 0.959 for all graphs).

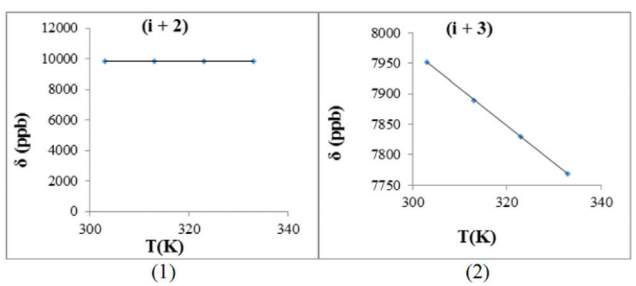

Fig. 12 The hydrogen bond investigation with thermal coefficient plots for each amide of *cis*-4b, [Bz(NO)PMeIVQ]. (Solvent: DMSO-d_6), (temperature: 293–333 K): (1) HN-Val ($-\Delta\delta/\Delta T$ = 0 ppb K^{-1}), (2) HN-Gln ($-\Delta\delta/\Delta T$ = 6.11 ppb K^{-1}) (R^2 > 0.999 for all graphs) (graphs for *trans*-**4b** are available in the ESI‡).

amides appeared in a region that is known for acid functional groups and this gives strong evidence for the acidic character of such amides. The ΔpK_a value for this system (amide and *N*-oxide) is expected to be low. It is important to note that ΔpK_a is directly related to temperature according to the Van't Hoff and Helmholtz equations.

With this background in mind, the amide proton NMR shifts were measured at different temperatures in order to determine the hydrogen bond character between the amide proton and the *N*-oxide oxygen atom. For *trans*-**1b**, [Bz(NO)-PGNF], the $-\Delta\delta/\Delta T$ graphs are presented in Fig. 9. The hydrogen bonding interaction between the amide proton (i + 1) and the *N*-oxide oxygen renders a positive slope (gradient = 2.64). This result is typical of normal acid–base equilibrium behaviour.[97]

The slopes of these graphs for normal peptides are usually negative.[91–96] The positive slope of this gradient (i + 1) suggests that the proton transfer in this system was temperature sensitive and the down field proton shift (≈10 ppm) suggests that the amide proton has probably started to transfer to the acceptor atom (*N*-oxide oxygen). There are two opposing factors playing a role in this case. First, the ΔpK_a value is directly proportional to the temperature and this causes the amide proton (i + 1) to be transferred to the *N*-oxide oxygen atom. Second, the glycine residue causes less steric hindrance and provides greater flexibility to the peptide at higher temperatures. This flexible nature makes transfer of the amide proton more difficult/less possible.

The non-hydrogen-bonded amides (i + 2 and i + 3) seem to be slightly more shielded at higher temperatures with the

expected negative slopes (4.56 and 4.50). These values are typical of peptide amide protons in the absence of hydrogen bonding interactions.[91–96]

The $-\Delta\delta/\Delta T$ plots for both of the backbone amides of *trans*-**2b**, [Bz(NO)PMeGNF], are presented in Fig. 10. The hydrogen bonding interaction between the amide proton (i + 2) and the *N*-oxide oxygen gave a positive slope (gradient = 1.49). This value verifies that the hydrogen bond was not as strong as for **1b** (i + 1). The observed gradient for the (i + 1) system in **1b** is higher (gradient = 2.64) than for the (i + 2) system in **2b** (gradient = 1.49); the latter exhibits less temperature dependence, most possibly due to the more flexible nature of the larger NO-β-turn structure.

An important difference between the (i + 2) data for **1b** and **2b** is that the sign of the slopes is indicative of substantial hydrogen bonding for **2b**. Blocking of the (i + 1) amide proton through N-methylation therefore induces stronger hydrogen bonding interactions between the (i + 2) amide proton and the *N*-oxide oxygen atom. The unusual positive slope of the HN-Asn plot is related to an acid–base equilibrium between the amide proton and the *N*-oxide moiety. For the next amide (i + 3) of **2b**, this slope was negative (-7.29 ppb K^{-1}) suggesting that this NH does not participate in a hydrogen bonding interaction with NO.

The $-\Delta\delta/\Delta T$ plots for the backbone amides of *trans*-**3b**, [Bz(NO)PIVQ], are presented in Fig. 11. The hydrogen bonding interaction between the amide proton (i + 1) and the *N*-oxide oxygen resulted in a positive slope (gradient = 0.66). This small value combined with the deshielding experienced by this proton (appeared at about 12 ppm) suggests that the proton is being completely transferred from the donor to the acceptor. In other words, it suggests hydrogen bonding in the absence of acid–base equilibrium between the *N*-oxide moiety and the amide proton. In comparison with **1b**, the slope for the (i + 1) system of **3b** is more shallow. A potential reason for that is the more rigid nature of peptide **3b**, allowing for substantial transfer of the amide proton to NO, even at higher temperatures. It therefore becomes an entropy driven effect where the corresponding system in **3b** is more ordered.

The sign and values of the slopes of *trans*-**3b** for (i + 2) and (i + 3) clearly show that these backbone amide protons are not involved in hydrogen bonding interactions.

The case of **4b** turned out to be unusual in terms of the behaviour observed so far. The proton NMR spectrum for *trans*-**4b** exhibits no unusual deshielding of any of the amide protons (Fig. 8). On the other hand, the *cis*-isomer displays an amide proton at about 10 ppm. The $-\Delta\delta/\Delta T$ plots for *cis*-**4b**, [Bz(NO)PMeIVQ], illustrate a hydrogen bonding interaction between the NH (i + 2) and the *N*-oxide oxygen, but it is not as strong as that observed for the corresponding system in **3b** (Fig. 12). The slope of this system is zero, indicating a strong hydrogen bond, but in the absence of acid–base equilibrium.

The sign and value of the slope of *cis*-**4b** for (i + 3) indicates that the protons do not experience hydrogen bonding interactions, similar to the non-hydrogen bonded amides presented before.

In summary, the results from the NMR spectroscopic studies show that the NO modification leads to a strong hydrogen bond with the closest backbone NH. Peptides **1b** and **3b** presented NO-γ-turns as a *trans*-isomer. N-methylation of the first amide, as in peptides **2b** and **4b**, leads to novel NO-β-turns. Utilization of N-methylated amino acids in the designed backbones leads to *cis*- and *trans*-isomerization. Peptide **2b**, with less sterically hindered residues, tends to form a NO-β-turn through the *trans*-isomer (*cis*/*trans* ratio 29/71). In contrast, peptide **4b** creates the NO-β-turn *via* the *cis*-isomer (*cis*/*trans* ratio 77/23), because the *cis*-isomer is less sterically hindered than the *trans*-isomer.

Computational studies

After NMR spectroscopic characterization of these series of molecules by NMR, we undertook a computational investigation to gain additional understanding of the structure of these novel kinds of turns. The free distance of the hydrogen bonding interactions between the NH proton and the NO oxygen for γ- and β-turns was calculated by density functional theory [B3LYP/6-31+G(d)] using a DMSO solvation model.

Compounds **1b** and **3b** displayed NO-γ-turns (compound **1b** is shown in Fig. 13). The calculated distance between NH (i + 1) and oxygen of NO is 1.76 Å. In the case of **3b**, the corresponding calculated distance was 1.71 Å.

The optimized structure for *trans*-**2b** is provided in Fig. 14, indicating the intramolecular hydrogen bonding interactions between NH (i + 2) and *N*-oxide oxygen that illustrates the NO-β-turn.

The optimized geometry for *cis*-**4b** is presented in Fig. 15, indicating a hydrogen bonding interaction between NH (i + 2) and *N*-oxide oxygen. The relative short distance between the hydrogen bond donor and the acceptor (2.35 Å) suggests a tight turn in this molecule.

The presence of sterically hindered amino acids normally prevents the formation of hydrogen bonding interactions for weak acceptors such as carbonyl groups. However, it can be concluded that for a strong acceptor like *N*-oxide oxygen when it is combined with N-methylation of the (i + 1) amide proton, the existence of bulky side chains in amino acids appears to

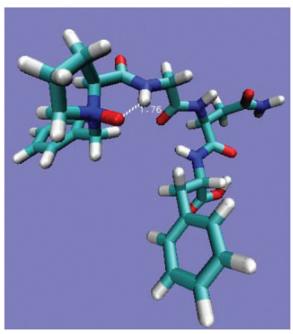

Fig. 13 The NO-γ-turn and the presence of the intramolecular hydrogen bonding interaction in the optimized structure of **1b**. (The 3D structures of **1b** and **3b** are available in the ESI‡.)

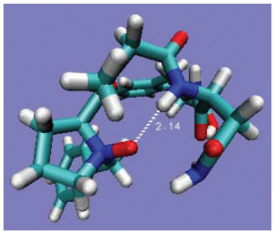

Fig. 14 The NO-β-turn and the presence of intramolecular hydrogen bonding in the optimized structure of *trans*-**2b**. (The 3D structure of *trans*-**2b** is available in the ESI‡.)

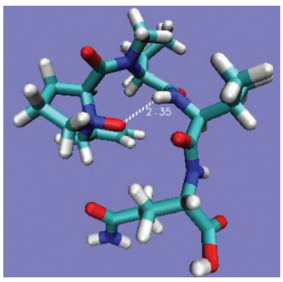

Fig. 15 The NO-β-turn intramolecular interaction presented in the optimized structure of *cis*-**4b**. (The 3D structure of *cis*-**4b** is available in the ESI‡.)

induce a stronger hydrogen bonding interaction for the $(i + 2)$ system. The possibility of more prominent *cis*-conformations is also possible.

Conclusion

A series of novel proline *N*-oxide peptides including less sterically hindered residues as well as sterically hindered amino acids were synthesised. NMR studies appear to reveal that a proline *N*-oxide residue enforces hydrogen bonding interactions with neighbouring backbone amide protons. Hydrogen bonding with the $(i + 1)$ amide bond leads to a quasi γ-turn which we named as a NO-γ-turn. When the $(i + 1)$ amino acid is N-methylated, the peptide experience *cis*- and *trans*-isomerization around this bond and instead forms a novel quasi β-turn, correspondingly named as a NO-β-turn. Computational results support the proposed explanation of the experimental results. Overall, *N*-oxide and N-methylated residue modifications allow the peptide backbone to assume predictable folded conformations, an outcome that may play an important role in *de novo* modulation of peptide secondary structures.

Experimental section

Fmoc-protected amino acids, CTC resin and HBTU were purchased from GL-Biochem (Shanghai, China). HPLC-grade CH_3CN, MeOH, peptide synthesis-grade DMF, CH_2Cl_2, DIEA, TFA and all other reagents were purchased from Sigma-Aldrich (Germany). Analytical reversed-phase HPLC was performed on a C_{18} column (4.6 × 150 mm, 5 μm, YMC Triart, UK) with a LC-MS 2020A system (Shimadzu, Kyoto, Japan). Solvents A and B were 0.01% (v/v) formic acid in Milli-Q water and CH_3CN, respectively. Elution was achieved with linear 0–90% gradients of solvent B to A over 15 minutes at 1 ml min^{-1} flow rate, with UV detection at 200 nm. Preparative HPLC was performed with a C_8 column (150 × 21.2 mm, 10 μm, Hichrom) attached to a Shimadzu LC-8A instrument. Solvents A and B were 0.1% formic acid (v/v) in water and MeOH, respectively, and a linear gradient of solvent B to A over 40 minutes at 15 mL min^{-1} flow rate was applied. The UV detection wavelength was set at 200 nm. Purified fractions (>95%) by HPLC were pooled and lyophilized on a Virtis SP scientific Sentry 2.0. Purified peptides and conjugates were characterized by HRMS, on a BrukermicrOTOF-Q II instrument operating at ambient temperature with 1 ppm sample. DMSO-d_6 was used as a solvent for sample preparation of NMR. ^{1}H NMR, ^{13}C NMR, COSY, HSQC, HMBC and ROESY experiments were performed at ambient temperature on an AVANCE III 600 MHz NMR (Bruker, Germany). The chemical shifts are expressed in ppm downfield from TMS as the internal standard. To achieve better resolution in the NMR spectra, the water peak was suppressed in necessary cases.

General procedure for the synthesis of the tetrapeptides

Peptides were manually synthesized on a 0.1 mmol scale on CTC resin (0.6 mmol g^{-1}). The resin was activated using 10% thionylchloride (v/v) in dry DCM, after which incorporation of the C-terminal amino acids was performed with a minimum of four equivalents of Fmoc-amino acid and six equivalents of DIEA in dry DCM for 3 hours. Elongation of the peptide chains was achieved following standard Fmoc protocols. The coupling conditions were 5-fold molar excess of Fmoc-amino acid and HBTU and double molar excess of DIEA in DMF. Deprotection was achieved with 20% piperidine in DMF (3 × 10 min). Coupling of *N*-benzylproline was achieved employing the same method. After chain assembly, total deprotection and cleavage were carried out with TFA–DCM (40 : 60) for one hour and the peptides were precipitated by adding chilled diethyl ether. After evaporation to dryness, the solid forms of the crude peptides were obtained. The crude peptides were purified *via* semi preparative HPLC and characterized by NMR and HRMS.

General procedure for the preparation of *N*-oxide tetrapeptides

Crude peptide (0.1 mmol) and K_2CO_3 (2.5 equiv.) were dissolved in dry DCM (10 ml). M-CPBA (1.6 equiv.) was added to a cooled solution mixture (−72 °C). The reaction was stirred for four hours under the same conditions and warmed up to room temperature over two hours. Finally, the solvent was evaporated and the product was purified by preparative HPLC and characterized by NMR and HRMS.

Molecular modelling method

The conformational models of four cases that demonstrate NO-γ-turns and NO-β-turns were investigated using

Gaussian09.[100] These compounds were *trans*-1b-γ-turn, *trans*-**3b**-γ-turn, *trans*-**2b**-β-turn and *cis*-**4b**-β-turn. The structures were first optimized (PM6)[101] with constrained bond lengths of about 3 Å between the corresponding amide proton and the oxygen of NO. After that, the optimized structures were again optimized without any constraints, using B3LYP[102,103] with the 6-31+G(d) basis set in DMSO (ε = 46.826) as an intrinsic solvent using the polarizable continuum model (PCM)[104] The second-derivative analytical vibration frequency of each optimized structure was calculated at the same theoretical level to find the stationary point without imaginary frequencies.

Acknowledgements

We thank the National Research Foundation, South Africa and UKZN for financial support. We are also grateful for the helpful support of CHPC (http://www.chpc.ac.za) for their computational resources.

References

1 A. Mullard, *Nat. Rev. Drug Discovery*, 2013, **12**, 87–90.
2 P. Y. Muller and M. N. Milton, *Nat. Rev. Drug Discovery*, 2012, **11**, 751–761.
3 M. Saffran, G. S. Kumar, C. Savariar, J. C. Burnham, F. Williams and D. C. Neckers, *Science*, 1986, **233**, 1081–1084.
4 R. I. Mahato, A. S. Narang, L. Thoma and D. D. Miller, *Crit. Rev. Ther. Drug Carrier Syst.*, 2003, **20**, 153–214.
5 T. Bruckdorfer, O. Marder and F. Albericio, *Curr. Pharm. Biotechnol.*, 2004, **5**, 29–43.
6 J. A. Fix, *Pharm. Res.*, 1996, **13**, 1760–1764.
7 M. Saffran, B. Pansky, G. C. Budd and F. E. Williams, *J. Controlled Release*, 1997, **46**, 89–98.
8 W. L. Cody, J. X. He, M. D. Reily, S. J. Haleen, D. M. Walker, E. L. Reyner, B. H. Stewart and A. M. Doherty, *J. Med. Chem.*, 1997, **40**, 2228–2240.
9 J. Chatterjee, D. Mierke and H. Kessler, *J. Am. Chem. Soc.*, 2006, **128**, 15164–15172.
10 E. Biron, J. Chatterjee, O. Ovadia, D. Langenegger, J. Brueggen, D. Hoyer, H. A. Schmid, R. Jelinek, C. Gilon, A. Hoffman and H. Kessler, *Angew. Chem., Int. Ed.*, 2008, **47**, 2595–2599.
11 P. P. Bose, U. Chatterjee, I. Hubatsch, P. Artursson, T. Govender, H. G. Kruger, M. Bergh, J. Johansson and P. I. Arvidsson, *Bioorg. Med. Chem.*, 2010, **18**, 5896–5902.
12 D. E. Stewart, A. Sarkar and J. E. Wampler, *J. Mol. Biol.*, 1990, **214**, 253–260.
13 A. Radzicka, S. A. Acheson and R. Wolfenden, *Bioorg. Chem.*, 1992, **20**, 382–386.
14 E. S. Eberhardt, N. Panasik and R. T. Raines, *J. Am. Chem. Soc.*, 1996, **118**, 12261–12266.
15 M. S. Weiss, A. Jabs and R. Hilgenfeld, *Nat. Struct. Biol.*, 1998, **5**, 676.
16 A. Jabs, M. S. Weiss and R. Hilgenfeld, *J. Mol. Biol.*, 1999, **286**, 291–304.
17 D. Pal and P. Chakrabarti, *J. Mol. Biol.*, 1999, **294**, 271–288.
18 B. Wathen and Z. Jia, *J. Proteome Res.*, 2008, **7**, 145–153.
19 N. Sewald and H.-D. Jakubke, *Peptides: Chemistry and Biology*, Wiley, Illustrated edn, 2009.
20 C. Grathwohl and K. Wuthrich, *Biopolymers*, 1976, **15**, 2025–2041.
21 G. Fischer, H. Bang, E. Berger and A. Schellenberger, *Biochim. Biophys. Acta*, 1984, **791**, 87–97.
22 R. L. Stein, *Adv. Protein Chem.*, 1993, **44**, 1–24.
23 A. Yaron and F. Naider, *Crit. Rev. Biochem. Mol. Biol.*, 1993, **28**, 31–81.
24 S. Fischer, R. L. Dunbrack and M. Karplus, *J. Am. Chem. Soc.*, 1994, **116**, 11931–11937.
25 W. A. Houry and H. A. Scheraga, *Biochemistry*, 1996, **35**, 11719–11733.
26 K. Mikoshiba and A. Lajtha, *Handbook of Neurochemistry and Molecular Neurobiology: Neural Signaling Mechanisms*, Springer, 2009.
27 J. L. Kofron, P. Kuzmic, V. Kishore, E. Colon-Bonilla and D. H. Rich, *Biochemistry*, 1991, **30**, 6127–6134.
28 M. D. Pluth, R. G. Bergman and K. N. Raymond, *J. Org. Chem.*, 2008, **73**, 7132–7136.
29 S. C. R. Lummis, D. L. Beene, L. W. Lee, H. A. Lester, R. W. Broadhurst and D. A. Dougherty, *Nature*, 2005, **438**, 248–252.
30 K. M. Thomas, D. Naduthambi and N. J. Zondlo, *J. Am. Chem. Soc.*, 2006, **128**, 2216–2217.
31 D. A. Case, T. E. Cheatham, T. Darden, H. Gohlke, R. Luo, K. M. Merz, A. Onufriev, C. Simmerling, B. Wang and R. J. Woods, *J. Comput. Chem.*, 2005, **26**, 1668–1688.
32 C. J. White and A. K. Yudin, *Nat. Chem.*, 2011, **3**, 509–524.
33 S. A. W. Gruner, V. Truffault, G. Voll, E. Locardi, M. Stöckle and H. Kessler, *Chem. – Eur. J.*, 2002, **8**, 4365–4376.
34 G. V. M. Sharma, K. R. Reddy, P. R. Krishna, A. R. Sankar, K. Narsimulu, S. K. Kumar, P. Jayaprakash, B. Jagannadh and A. C. Kunwar, *J. Am. Chem. Soc.*, 2003, **125**, 13670–13671.
35 S. Chandrasekhar, M. S. Reddy, B. Jagadeesh, A. Prabhakar, M. H. V. R. Rao and B. Jagannadh, *J. Am. Chem. Soc.*, 2004, **126**, 13586–13587.
36 G. V. M. Sharma, V. B. Jadhav, K. V. S. Ramakrishna, P. Jayaprakash, K. Narsimulu, V. Subash and A. C. Kunwar, *J. Am. Chem. Soc.*, 2006, **128**, 14657–14668.
37 B. Jagannadh, M. S. Reddy, C. L. Rao, A. Prabhakar, B. Jagadeesh and S. Chandrasekhar, *Chem. Commun.*, 2006, 4847–4849.
38 B. Jagadeesh, A. Prabhakar, G. D. Sarma, S. Chandrasekhar, G. Chandrashekar, M. S. Reddy and B. Jagannadh, *Chem. Commun.*, 2007, 371–373.
39 B. Jagadeesh, M. U. Kiran, A. Sudhakar and S. Chandrasekhar, *Chem. – Eur. J.*, 2009, **15**, 12592–12595.

40 A. Sharma, S. Sharma, R. P. Tripathi and R. S. Ampapathi, *J. Org. Chem.*, 2012, **77**, 2001–2007.
41 N. Berova, P. L. Polavarapu, K. Nakanishi and R. W. Woody, *Comprehensive Chiroptical Spectroscopy, Applications in Stereochemical Analysis of Synthetic Compounds, Natural Products, and Biomolecules*, Wiley, 2012.
42 C. Venkatac, *Biopolymers*, 1968, **6**, 1425–1436.
43 G. Nemethy and M. P. Printz, *Macromolecules*, 1972, **5**, 755–758.
44 B. W. Matthews, *Macromolecules*, 1972, **5**, 818–819.
45 P. N. Lewis, F. A. Momany and H. A. Scheraga, *Biochim. Biophys. Acta*, 1973, **303**, 211–229.
46 A. S. Kolaskar, A. V. Lakshminarayanan, K. P. Sarathy and V. Sasisekharan, *Biopolymers*, 1975, **14**, 1081–1094.
47 G. D. Rose, L. M. Gierasch and J. A. Smith, *Adv. Protein Chem.*, 1985, **37**, 1–109.
48 D. K. Chalmers and G. R. Marshall, *J. Am. Chem. Soc.*, 1995, **117**, 5927–5937.
49 K. Mohle, M. Gussmann and H. J. Hofmann, *J. Comput. Chem.*, 1997, **18**, 1415–1430.
50 F. Albericio, P. I. Arvidson, K. Bisetty, E. Giral, T. Govender, S. Jali, P. Kongsaeree, H. G. Kruger and S. Prabpai, *Chem. Biol. Drug Des.*, 2008, **71**, 125–130.
51 K. Bisetty, F. J. Corcho, J. Canto, H. G. Kruger and J. J. Perez, *J. Mol. Struct. (THEOCHEM)*, 2006, **759**, 145–157.
52 K. Bisetty, F. J. Corcho, J. Canto, H. G. Kruger and J. J. Perez, *J. Pept. Sci.*, 2006, **12**, 92–105.
53 I. A. O'Neil, N. D. Miller, J. Peake, J. V. Barkley, C. M. R. Low and S. B. Kalindjian, *Synlett*, 1993, 515–518.
54 I. A. O'Neil, N. D. Miller, J. V. Barkley, C. M. R. Low and S. B. Kalindjian, *Synlett*, 1995, 619–621.
55 E. G. Hutchinson and J. M. Thornton, *Protein Sci.*, 1994, **3**, 2207–2216.
56 C. Zheng and L. Kurgan, *BMC Bioinformatics*, 2008, **9**, 430–443.
57 K. Guruprasad and S. Rajkumar, *J. Biosci.*, 2000, **25**, 143–156.
58 T. H. Pham, K. Satou and T. B. Ho, *Genome Inf. Int. Conf. Genome Inf.*, 2003, **14**, 196–205.
59 M. Billeter, W. Braun and K. Wuethrich, *J. Mol. Biol.*, 1982, **155**, 321–346.
60 Y. Xiong, D. Juminaga, G. V. T. Swapna, W. J. Wedemeyer, H. A. Scheraga and G. T. Montelione, *Protein Sci.*, 2000, **9**, 421–426.
61 K.-y. Hung, P. W. R. Harris and M. A. Brimble, *J. Org. Chem.*, 2010, **75**, 8728–8731.
62 B. Gao, Y. Wen, Z. Yang, X. Huang, X. Liu and X. Feng, *Adv. Synth. Catal.*, 2008, **350**, 385–390.
63 T. Naicker, P. I. Arvidsson, H. G. Kruger, G. E. M. Maguire and T. Govender, *Eur. J. Org. Chem.*, 2011, 6923–6932.
64 M. Breznik, S. G. Grdadolnik, G. Giester, I. Leban and D. Kikelj, *J. Org. Chem.*, 2001, **66**, 7044–7050.
65 J. F. Brandts, H. R. Halvorson and M. Brennan, *Biochemistry*, 1975, **14**, 4953–4963.
66 M. Oka, G. T. Montelione and H. A. Scheraga, *J. Am. Chem. Soc.*, 1984, **106**, 7959–7969.
67 G. Fischer and F. X. Schmid, *Biochemistry*, 1990, **29**, 2205–2212.
68 T. Kiefhaber, H. H. Kohler and F. X. Schmid, *J. Mol. Biol.*, 1992, **224**, 217–229.
69 R. L. Baldwin, *Bioessays*, 1994, **16**, 207–210.
70 R. W. Dodge and H. A. Scheraga, *Biochemistry*, 1996, **35**, 1548–1559.
71 L. Birolo, V. N. Malashkevich, G. Capitani, L. F. De, A. Moretta, J. N. Jansonius and G. Marino, *Biochemistry*, 1999, **38**, 905–913.
72 L. Jin, B. Stec and E. R. Kantrowitz, *Biochemistry*, 2000, **39**, 8058–8066.
73 U. Reimer and G. Fischer, *Biophys. Chem.*, 2002, **96**, 203–212.
74 C. Dugave and L. Demange, *Chem. Rev.*, 2003, **103**, 2475–2532.
75 A. H. Andreotti, *Biochemistry*, 2003, **42**, 9515–9524.
76 E. A. Meyer, R. K. Castellano and F. Diederich, *Angew. Chem., Int. Ed.*, 2003, **42**, 1210–1250.
77 R.-J. Guan, Y. Xiang, X.-L. He, C.-G. Wang, M. Wang, Y. Zhang, E. J. Sundberg and D.-C. Wang, *J. Mol. Biol.*, 2004, **341**, 1189–1204.
78 S. Lorenzen, B. Peters, A. Goede, R. Preissner and C. Frommel, *Proteins*, 2005, **58**, 589–595.
79 J. Leis, K. D. Klika and M. Karelson, *Tetrahedron*, 1998, **54**, 7497–7504.
80 J. Zhang and M. W. Germann, *Biopolymers*, 2011, **95**, 755–762.
81 H. Kessler, *Angew. Chem., Int. Ed. Engl.*, 1970, **9**, 219–235.
82 F. Piriou, K. Lintner, S. Fermandjian, P. Fromageot, M. C. Khosla, R. R. Smeby and F. M. Bumpus, *Proc. Natl. Acad. U. S. A.*, 1980, **77**, 82–86.
83 B. Laufer, J. Chatterjee, A. O. Frank and H. Kessler, *J. Pept. Sci.*, 2009, **15**, 141–146.
84 B. Laufer, A. O. Frank, J. Chatterjee, T. Neubauer, C. Mas-Moruno, G. Kummerloewe and H. Kessler, *Chem. – Eur. J.*, 2010, **16**, 5385–5390.
85 M. Goodman, F. Chen and C.-Y. Lee, *J. Am. Chem. Soc.*, 1974, **96**, 1479–1484.
86 G. Scherer, M. L. Kramer, M. Schutkowski, U. Reimer and G. Fischer, *J. Am. Chem. Soc.*, 1998, **120**, 5568–5574.
87 S. M. N. Crawford, A. N. Taha, N. S. True and C. B. LeMaster, *J. Phys. Chem. A*, 1997, **101**, 4699–4706.
88 J. B. Henrickson, D. J. Cram and G. S. Hammond, *Organic Chemistry*, McGraw-Hill, New York, 3rd edn, 1970.
89 H. G. Kruger, *J. Mol. Struct. (THEOCHEM)*, 2002, **577**, 281–285.
90 C. Dugave, *Cis-trans Isomerization in Biochemistry*, Wiley, 2006.
91 A. Aubry, M. T. Cung and M. Marraud, *J. Am. Chem. Soc.*, 1985, **107**, 7640–7647.
92 C. Toniolo, G. M. Bonora, G. Stavropoulos, P. Cordopatis and D. Theodoropoulos, *Biopolymers*, 1986, **25**, 281–289.

93 A. Aubry, J. P. Mangeot, J. Vidal, A. Collet, S. Zerkout and M. Marraud, *Int. J. Pept. Protein Res.*, 1994, **43**, 305–311.
94 S. Sakakibara, *Biopolymers*, 1995, **37**, 17–28.
95 S. Prasad, R. B. Rao and P. Balaram, *Biopolymers*, 1995, **35**, 11–20.
96 D. Ranganathan, V. Haridas, S. Kurur, A. Thomas, K. P. Madhusudanan, R. Nagaraj, A. C. Kunwar, A. V. S. Sarma and I. L. Karle, *J. Am. Chem. Soc.*, 1998, **120**, 8448–8460.
97 R. Langner and G. Zundel, *Can. J. Chem.*, 2001, **79**, 1376–1380.
98 P. Huyskens and T. Zeegers-Huyskens, *J. Chim. Phys. Phys.–Chim. Biol.*, 1964, **61**, 81–86.
99 P. Huyskens and G. Hernandez, *Ind. Chim. Belge*, 1973, **38**, 1237–1247.
100 G. W. Frisch, H. B. Schlegel, G. E. Scuseria, M. A. Robb, J. R. Cheeseman and J. A. Montgomery Jr., T. Vreven, K. N. Kudin, J. C. Burant, J. M. Millam, S. S. Iyengar, J. Tomasi, V. Barone, B. Mennucci, M. Cossi, G. Scalmani, N. Rega, G. A. Petersson, H. Nakatsuji, M. Hada, M. Ehara, K. Toyota, R. Fukuda, J. Hasegawa, M. Ishida, T. Nakajima, Y. Honda, O. Kitao, H. Nakai, M. Klene, X. Li, J. E. Knox, H. P. Hratchian, J. B. Cross, V. Bakken, C. Adamo, J. Jaramillo, R. Gomperts, R. E. Stratmann, O. Yazyev, A. J. Austin, R. Cammi, C. Pomelli, J. W. Ochterski, P. Y. Ayala, K. Morokuma, G. A. Voth, P. Salvador, J. J. Dannenberg, V. G. Zakrzewski, S. Dapprich, A. D. Daniels, M. C. Strain, O. Farkas, D. K. Malick, A. D. Rabuck, K. Raghavachari, J. B. Foresman, J. V. Ortiz, Q. Cui, A. G. Baboul, S. Clifford, J. Cioslowski, B. B. Stefanov, G. Liu, A. Liashenko, P. Piskorz, I. Komaromi, R. L. Martin, D. J. Fox, T. Keith, M. A. Al-Laham, C. Y. Peng, A. Nanayakkara, M. Challacombe, P. M. W. Gill, B. Johnson, W. Chen, M. W. Wong, C. Gonzalez and J. A. Pople, *R. A. Gaussian 09 and M. J. T*, Gaussian, Inc., Wallingford CT, 2009.
101 J. J. P. Stewart, *J. Mol. Model*, 2007, **13**, 1173–1213.
102 J. P. Perdew and A. Ruzsinszky, *Int. J. Quantum Chem.*, 2010, **110**, 2801–2807.
103 K. Burke, *J. Chem. Phys.*, 2012, 136.
104 J. Tomasi, B. Mennucci and R. Cammi, *Chem. Rev.*, 2005, **105**, 2999–3093.